

Modeling Total Solar Irradiance with San Fernando Observatory Ground-Based Photometry: Comparison with ACRIM, PMOD, and RMIB Composites

G.A. Chapman · A.M. Cookson · D.G. Preminger

Received: 7 May 2012 / Accepted: 16 January 2013 / Published online: 6 February 2013
© Springer Science+Business Media Dordrecht 2013

Abstract We model total solar irradiance (TSI) using photometric irradiance indices from the San Fernando Observatory (SFO), and compare our model with measurements compiled from different space-based radiometers. Space-based measurements of TSI have been obtained recently from ACRIM-3 on board the ACRIMSAT. These data have been combined with other data sets to create an ACRIM-based composite. From VIRGO on board the *Solar and Heliospheric Observatory* (SOHO) spacecraft two different TSI composites have been developed. The VIRGO irradiance data have been combined by the Davos group to create a composite often referred to as PMOD (Physikalisch-Meteorologisches Observatorium Davos). Also using data from VIRGO, the Royal Meteorological Institute of Belgium (RMIB) has created a separate composite TSI referred to here as the RMIB composite. We also report on comparisons with TSI data from the Total Irradiance Monitor (TIM) experiment on board the *Solar Radiation and Climate Experiment* (SORCE) spacecraft. The SFO model correlates well with all four experiments during the seven-year SORCE interval. For this interval, the squared correlation coefficient R^2 was 0.949 for SORCE, 0.887 for ACRIM, 0.922 for PMOD, and 0.924 for RMIB. Long-term differences between the PMOD, ACRIM, and RMIB composites become apparent when we examine a 21.5-year interval. We demonstrate that ground-based photometry, by accurately removing TSI variations caused by solar activity, is useful for understanding the differences that exist between TSI measurements from different spacecraft experiments.

Keywords Solar activity · Solar photometry · Total solar irradiance

1. Introduction

Space-based measurements of the total solar irradiance (TSI) have shown that the TSI varies in phase with the solar activity cycle. When the Sun is most active, magnetically, the irradiance is higher by about 0.1 % compared to quiet times, between cycle maxima. An important

G.A. Chapman (✉) · A.M. Cookson · D.G. Preminger
San Fernando Observatory, Department of Physics and Astronomy, California State University,
Northridge, Northridge, CA 91330, USA
e-mail: gchapman@csun.edu

task is to compare the different sets of data and, in so doing, improve our understanding of the source of variations. In a previous paper (Chapman, Cookson, and Preminger, 2012) we compared TSI data from the Total Irradiance Monitor (TIM; Kopp, Lawrence, and Rottman, 2005) experiment on board the *Solar Radiation and Climate Experiment* (SORCE) spacecraft with San Fernando Observatory (SFO) ground-based photometric data.

In this paper, we use a two-pronged approach. First, we compare 21.5 years of SFO data with three composites that bring together data from several spacecraft experiments. Second, we compare a shorter time interval of seven years of SFO data with TSI data from these same three experiments. The shorter interval coincides with the time period covered by the earlier study of the SORCE/TIM TSI. The TSI composites are the Active Cavity Radiometer Irradiance Monitor (ACRIM) composite, primarily from the ACRIM series of experiments (ACRIM-1, ACRIM-2, and ACRIM-3). The PMOD (Physikalisch-Meteorologisches Observatorium Davos) composite TSI is from Variability of Solar Irradiance and Gravity Oscillations (VIRGO; Fröhlich *et al.*, 1997) on the *Solar and Heliospheric Observatory* (SOHO) spacecraft as is the RMIB (Royal Meteorological Institute of Belgium) composite.

Previously, PMOD data were studied using irradiance proxies created from National Solar Observatory (NSO)/Kitt Peak and SOHO/MDI (Michelson Doppler Imager) magnetograms (Wenzler *et al.*, 2004, 2006). Krivova *et al.* (2003) found from a four-component model based on MDI magnetic field observations that they could fit VIRGO TSI with a multiple correlation coefficient, R , of 0.96 for a six-year interval from 1996 to 2002. Recently, Fontenla *et al.* (1999) created improved atmospheric models for determining improved models of spectral variations. Solanki and Krivova (2004), using Fröhlich's PMOD composite TSI (Fröhlich, 2003), found an R^2 of 0.92 for nine years of data from an analysis that used a TSI model based on the spectro-magnetograph at Kitt Peak. Mekaoui and Dewitte (2008) modeled the RMIB composite based on the VIRGO/DIARAD instrument as well as the ACRIM composite and the PMOD composite. They found an R^2 as high as 0.93. Mekaoui *et al.* (2010) also studied DIARAD data from the Solar Variable and Irradiance Monitor (SOVIM) on the International Space Station. Li *et al.* (2012) used the PMOD data to study fluctuations in TSI using a three-component model based on empirical mode decomposition and time-frequency analyses. Wenzler, Solanki, and Krivova (2009) produced a comparison of TSI composites from PMOD, ACRIM, and RMIB for the period from 1978 to 2003 that found no evidence of secular change in the solar minimum TSI. Ball *et al.* (2012) modeled the PMOD, ACRIM, and RMIB composite TSI observations using Kitt Peak continuum images and magnetograms and MDI images with their four-component Spectral And Total Irradiance REconstruction (SATIRE-S) model.

2. Description of the Data

In this paper, we construct empirical models of TSI data from the ACRIM composite, the PMOD composite, and the RMIB composite using photometric indices from SFO ground-based images. The ACRIM composite is described by Willson and Mordvinov (2003) and Willson (2004).¹ The PMOD composite is described by Fröhlich (2003, 2004, 2006).² The data from the RMIB composite are described by Mekaoui and Dewitte (2008) and Dewitte *et al.* (2004) and provided on the RMIB website.³

¹ACRIM composite TSI daily values from www.acrim.com/DataProducts.htm Version 11/11.

²PMOD TSI composite 24-h averages, from the Physikalisch-Meteorologisches Observatorium Davos website, ftp://ftp.pmodwrc.ch/pub/data/irradiance/composite/DataPlots/composite_d41_62_1212.dat.

³RMIB composite TSI is at <http://remotesensing.oma.be/en/2619579-Data.html>.

The SFO photometric indices are calculated from red and Ca II K-line images, which are obtained with interference filters at 672.3 nm and 393.4 nm, respectively. The red image is a single image, while the K-line image is the sum of two images separated by 7.5 min in order to reduce the amplitude of the p -mode signal. Photometric images from the Cartesian Full Disk Telescope no. 1 (CFDT1) have 512×512 pixels with 5.12 arcsec per pixel. A larger telescope, CFDT2, has 1024×1024 pixels with 2.5 arcsec per pixel (Chapman *et al.*, 2004). Both telescopes operate on a daily basis. The CFDT1 data begin in mid-1986 and continue to the present; the CFDT2 data begin in mid-1992 and also continue to the present time. On most days, weather permitting, data are obtained with both telescopes. The photometric indices from the two telescopes are highly correlated, showing the stability of the instruments over time. In this study, the red images used are from CFDT1.

The red filters in both telescopes have a bandpass of 10 nm, whereas the wide K-line filters from both telescopes have a bandpass of 1 nm. The K-line data from these images are combined into a composite in order to compensate for degradation in the filters and for their occasional replacement (Chapman, Dobias, and Arias, 2011). The photometric index, Σ_K (see Equation (2) below) is computed from this K-line composite (version 8).

The TSI values were regressed with two photometric indices, the red and Ca II K-line photometric sums (see Equations (1) and (2)), which were derived from daily data (Preminger, Walton, and Chapman, 2002). The Σ s are sums over *all* pixels on a contrast image. The contrast of each pixel is weighted by the observed, quiet-Sun limb darkening. Since these indices are from sums over all pixels there is no need to determine if a pixel is associated with a particular solar feature. Feature identification techniques were discussed by Ermolli, Berrilli, and Florio (2003), Fontenla and Harder (2005), Harvey and White (1999), Jones *et al.* (2008), Preminger, Walton, and Chapman (2001), and Ulrich *et al.* (2010).

Σ_r is determined from the red images as

$$\Sigma_r = \sum_i \frac{\Delta I_i}{I} \times \Phi_r(\mu_i). \quad (1)$$

Σ_K is determined from the K-line images as

$$\Sigma_K = \sum_i \frac{\Delta I_i}{I} \times \Phi_K(\mu_i). \quad (2)$$

The quantity $\frac{\Delta I_i}{I} = \frac{I_i}{I} - 1$ is the contrast of pixel i , and $\Phi_r(\mu_i)$ and $\Phi_K(\mu_i)$ denote the quiet-Sun limb darkening at pixel i . The quantity I in the denominator is the quiet-Sun intensity at pixel i , which is determined by a fit to the limb darkening using the median intensity in 20 annular rings (Walton *et al.*, 1998). Numerical simulation has shown that significant solar activity can have a small but measurable effect on the quiet-Sun level. We have not compensated for these small effects in this study. If biases exist in the SFO data, they will be apparent in the residuals of the fits to all three sets of spacecraft data.

3. Analysis of the Data

The ACRIM composite, the PMOD composite, and the RMIB composite TSIs were each made the dependent variable in the following regression equation:

$$\text{TSI} = S_0(1 + A\Sigma_r + B\Sigma_K). \quad (3)$$

The quantity S_0 is assumed to be the irradiance from the non-variable quiet Sun (Livingston *et al.*, 2005). The native scale of the Σ s is in parts per million (ppm) of the quiet Sun.

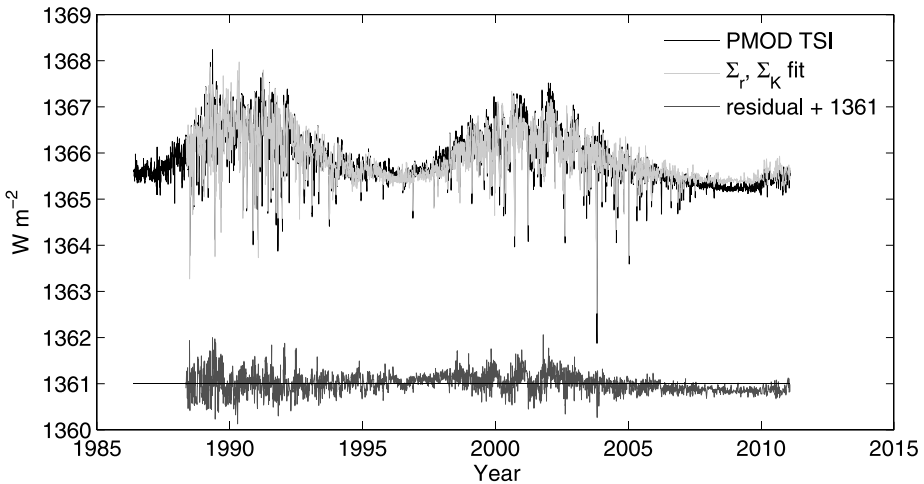


Figure 1 Plot of PMOD composite TSI and the SFO model given by Equation (3). The residuals are plotted offset so that zero is at 1361.0 W m^{-2} . Σ_r is from CFDT1 and Σ_K is from the K-line composite. The R^2 (squared correlation coefficient) is 0.877.

For ease of comparison, the regression coefficients A and B in Equation (3) have been converted from ppm to W m^{-2} by multiplying by 1361×10^{-6} . When there are sunspots on the disk, Σ_r is usually negative, although it can take on positive values when the facular/network area is large and the sunspot area is small. On the other hand, Σ_K is always positive but can become small when the Sun has relatively low activity.

The regression was carried out for two different groupings of the data. First, we used data starting on 14 November 1988 and ending on 4 May 2010, with the exception of RMIB which ended in 2009. The second grouping began on 2 March 2003 and ended on 4 May 2010 except for RMIB. This time interval corresponded to the time period for our analysis of the *SORCE/TIM* TSI reported in Chapman, Cookson, and Preminger (2012).

Figure 1 shows the fit of the SFO model of Equation (3) to the PMOD composite. The residuals are plotted below the data with 1361.0 W m^{-2} as the zero level. According to this PMOD composite, the minimum PMOD/TSI between cycles 22 and 23 and between cycles 23 and 24 are not at the same level. This is in disagreement with the SFO model. Figure 2 shows the fit to the PMOD composite with Σ_K replaced with the Mg II composite. During the period from about 2000 to 2003, there appears to be an annual signal in the residuals. A similar fluctuation was noted for 2001 in Figure 10 in Ball *et al.* (2012), where the model indices were calculated from the SATIRE-S model as applied to MDI images.

When a model is created based on SFO's Σ_r and the core/wing ratio of Mg II, essentially the same behavior is seen. This fit (seen in Figure 2) has a very slightly higher squared correlation coefficient R^2 of 0.88 compared with 0.877 in Figure 1.

Figure 3 shows the fit to the ACRIM composite TSI using Σ_r and Σ_K . Figure 4 shows the fit to the ACRIM TSI composite with Σ_K replaced with the Mg II composite. Figure 5 shows a plot of the fit to the RMIB TSI composite using Σ_r and Σ_K .

Figures 6, 7, and 8 show the fits to TSI for the seven-year period corresponding to the *SORCE* interval. The fits using Equation (3) are for the PMOD composite, the ACRIM composite, and the RMIB composite, respectively. The fit to the *SORCE* TSI is shown for the same interval in Figure 1 in Chapman, Cookson, and Preminger (2012). That fit gave an R^2 of 0.9495.

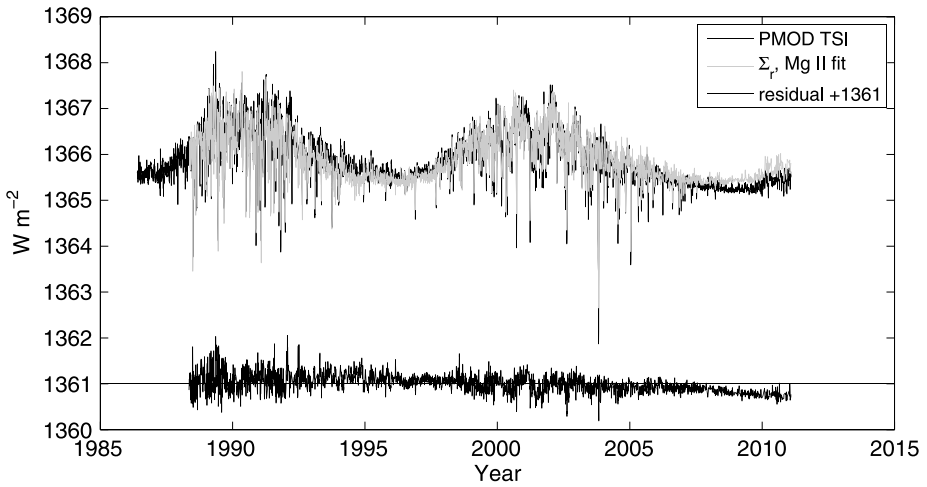


Figure 2 Plot of PMOD composite TSI and an SFO model using Σ_r and the Mg II core/wing ratio in place of Σ_K . R^2 is 0.88.

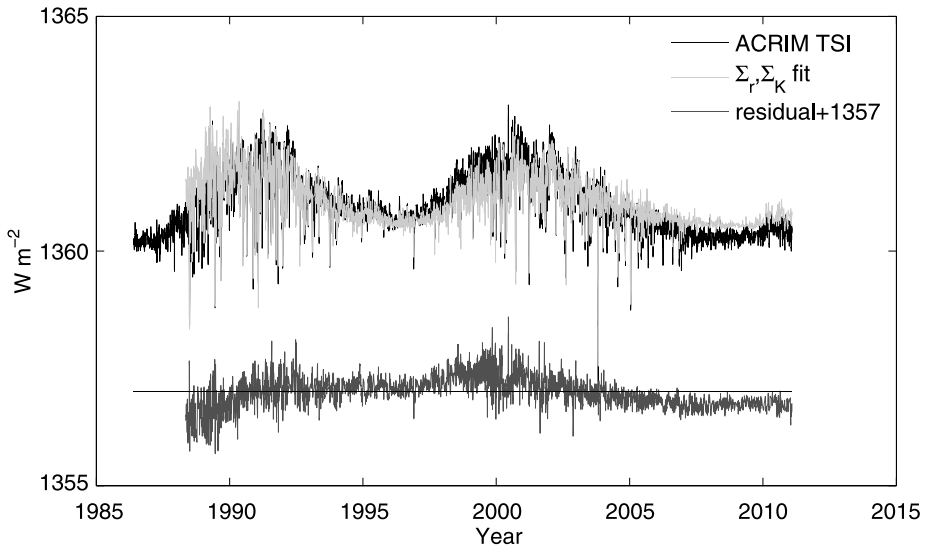


Figure 3 Plot of ACRIM composite TSI and the SFO model using Σ_r and Σ_K . R^2 is 0.737.

Figure 9 shows the reconstructed TSI based on the SFO indices Σ_r and Σ_K with the residuals from the individual fits shown below. This graph shows more clearly the differences in the residuals from the three TSI data sets. The RMIB and, especially, the PMOD show smaller long-term trends when compared with the ACRIM residuals.

In Table 1, the coefficients from Equation (3) are shown with their standard errors. S_0 represents the quiet-Sun irradiance with no activity. In all cases in Table 1, the coefficient B is based on the use of Σ_K . The root-mean-square (rms) of the residuals, σ , is in $W m^{-2}$.

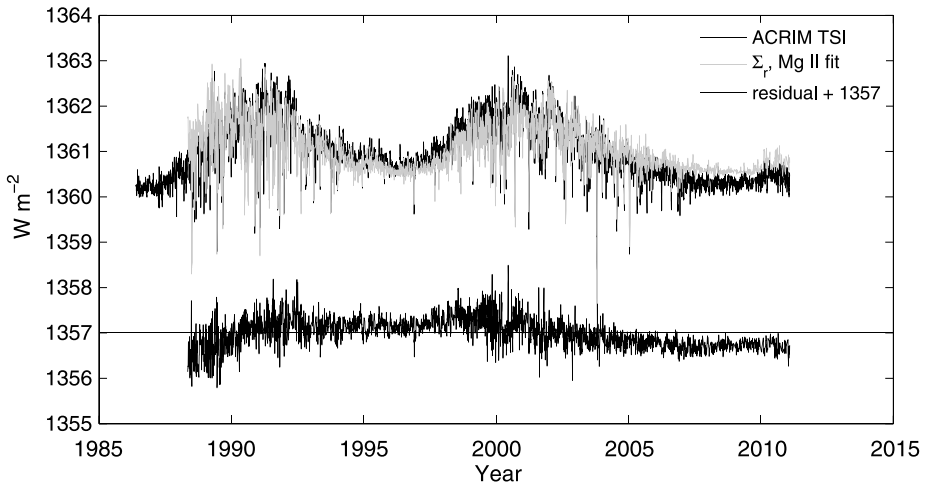


Figure 4 Plot of ACRIM composite TSI and the SFO model using Σ_r and the Mg II core/wing ratio in place of Σ_K . R^2 is 0.750.

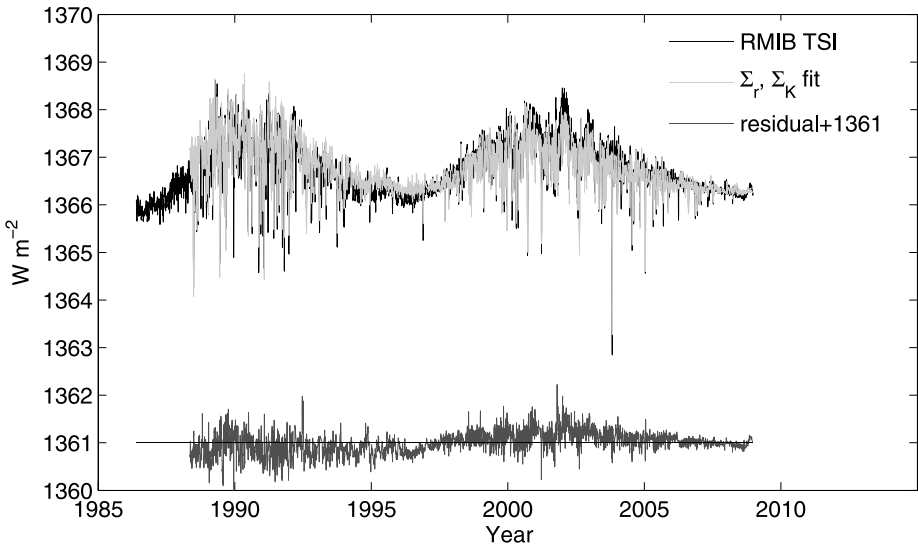


Figure 5 Plot of RMIB composite TSI and the SFO model using Σ_r and Σ_K . R^2 is 0.845.

These main results are summarized in Table 2. The quantity N is the number of data points that were included in the regression. The values of R^2 are so similar and so close to unity that we have included the F -statistic which may help the reader to better compare the quality of the fits. The F -statistic is defined as

$$F = \frac{R^2}{(1 - R^2)} \frac{(N - m)}{(m - 1)}, \tag{4}$$

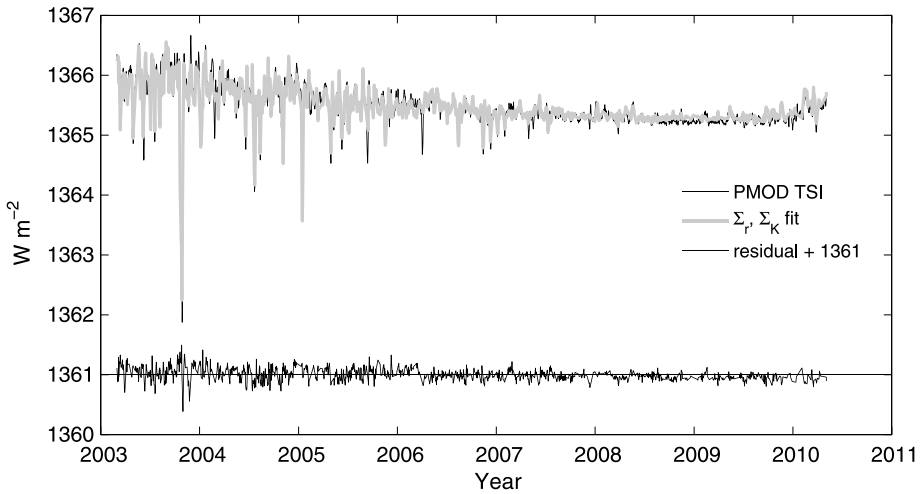


Figure 6 Plot of PMOD TSI and the SFO model using Σ_r and Σ_K for the 7-year interval. R^2 is 0.922.

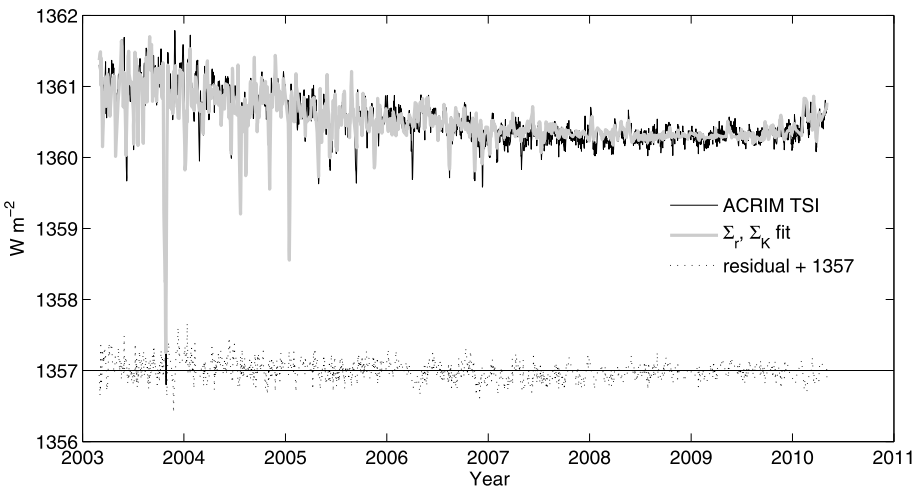


Figure 7 Plot of ACRIM TSI and the SFO model using Σ_r and Σ_K for the seven-year interval. R^2 is 0.887.

where R is the multiple regression coefficient, N is the number of data points, and m is the number of coefficients (Bevington and Robinson, 1992). The larger the value of the F -statistic for the same number of data points and the same number of coefficients, the better the fit. In column 3, modeled TSI data were regressed with spacecraft data for the whole interval for which processed SFO data exist. This interval is from mid-1988 through the end of 2011. In column 4, modeled TSI data were regressed with data for the interval during which SORCE data exist. The RMIB data set goes to the end of 2008, so the number of RMIB data points, given in Table 2, is less than those for ACRIM and PMOD.

Mekaoui and Dewitte (2008) regressed RMIB, PMOD, and ACRIM TSI using a three-component model similar to Equation (3) using the SFO Σ_r , the Mg II core-to-wing index, and the Mount Wilson magnetic plage index. For the three data sets they find an R^2 of 0.93,

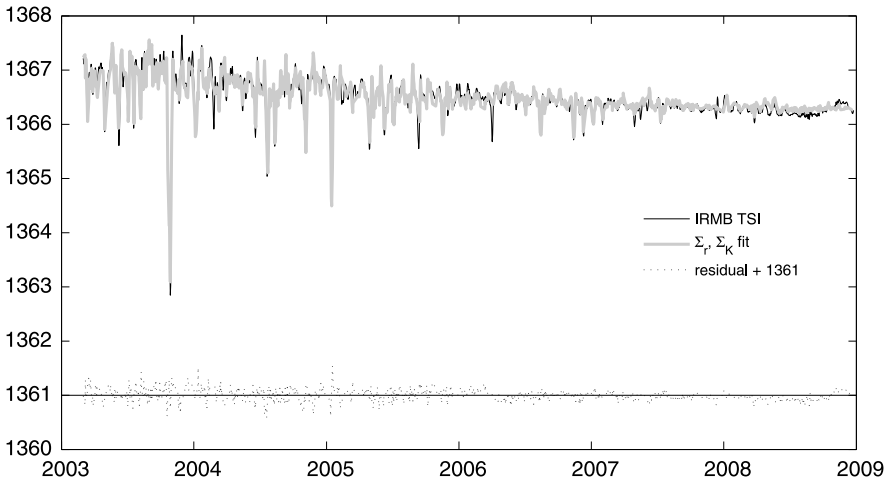


Figure 8 Plot of RMIB TSI versus the SFO model (Equation (3)) for the seven-year interval. R^2 is 0.924.

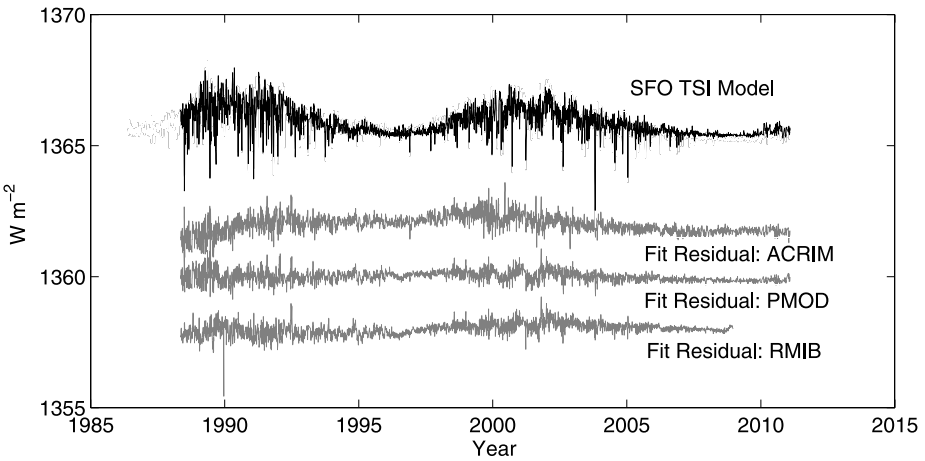


Figure 9 Summary plot of the SFO TSI reconstruction with the fit residuals for the three sets of spacecraft data.

0.86, and 0.75 for RMIB, PMOD, and ACRIM, respectively, for a ten-year period from 1996 to 2006. These results are similar to those presented here. The quiet-Sun irradiance, S_0 , for the ACRIM composite is very close to that found using SORCE data, 1360.5 *versus* 1360.8 $W m^{-2}$. The lower ACRIM quiet-Sun value compared to earlier published values is a result of new diffraction corrections for the ACRIM cavities (Willson, 2011). We now have two spacecraft experiments with a quiet-Sun TSI slightly less than 1361 $W m^{-2}$. This is a decrease of nearly 7 $W m^{-2}$ from the S_0 previously found using ACRIM-1 TSI data (Chapman *et al.*, 1992).

The time period covered in this paper is from shortly after the minimum of solar cycle 22 to just after the minimum between cycles 23 and 24, which was one of the longest minima in solar activity in many years.

Table 1 Regression coefficients and fit residuals (see Equation (3)).

Model	Coefficient	21.5 years	7 years
ACRIM composite	S_0 ($W m^{-2}$)	1360.5	1360.2
	A	0.991 ± 0.013	1.0382 ± 0.0125
	B	0.123 ± 0.0012	0.1470 ± 0.0015
	σ ($W m^{-2}$)	0.32	0.14
PMOD composite	S_0 ($W m^{-2}$)	1365.4	1365.2
	A	0.951 ± 0.007	1.0103 ± 0.0095
	B	0.120 ± 0.0007	0.1297 ± 0.0013
	σ ($W m^{-2}$)	0.20	0.10
RMIB composite	S_0 ($W m^{-2}$)	1366.2	1366.2
	A	0.976 ± 0.008	1.0490 ± 0.0102
	B	0.113 ± 0.0008	0.1280 ± 0.0015
	σ ($W m^{-2}$)	0.22	0.11

Table 2 Summary of main regression results.

Model	Parameter	21.5 years	7 years
ACRIM composite	R^2	0.737	0.887
	F	6530	5339
	N	4668	1365
Equation (3)	S_0	1360.5	1360.2
PMOD composite	R^2	0.877	0.922
	F	16601	8048
	N	4668	1365
Equation (3)	S_0	1365.3	1365.2
RMIB composite	R^2	0.845	0.924
	F	11959	7204
	N	4393	1188
Equation (3)	S_0	1366.2	1366.2
SORCE/ TIM	R^2		0.9495
	F		11751
	N		1253
	S_0		1360.81

4. Discussion and Conclusions

The TSI from ACRIM, PMOD, and RMIB were compared with a simple regression model using two indices from SFO that respond to sunspots, faculae, and network. The two indices were Σ_r (mostly sensitive to sunspots) and a composite Σ_K (mostly sensitive to faculae and network). The fits cover either 21.5 years or 7 years of data from shortly after the cycle 22 minimum through to the beginning of cycle 24.

The SFO indices fit each of the three spacecraft composites almost equally well. The PMOD results were slightly better than those using the ACRIM data, but the differences, especially for the seven-year interval, were quite small. The PMOD and RMIB results were especially close. In Table 1, the rms values of the residuals are very close to those given in Dewitte *et al.* (2004) based on results from a slightly different regression model. When Mg II data were substituted for the SFO Σ_K data, the results were nearly identical, which is not too surprising, as the SFO K-data correlate very well with the Mg II data (de Toma *et al.*, 2004).

The differences in the minima between cycles 22 and 23 (ca. 1996) and between cycles 23 and 24 (ca. 2008) are smaller for the PMOD composite than the ACRIM composite, as seen in Figures 1 and 3 or Figures 2 and 4. The multiple correlation coefficient found here was slightly higher than the one found by Solanki and Krivova (2004) and Wenzler *et al.* (2004). It was nearly the same as that found by Krivova *et al.* (2003) using VIRGO TSI modeled from MDI data and Ball *et al.* (2011) using SORCE TIM and MDI data. More recently, Ball *et al.* (2012) modeled the TSI from PMOD and RMIB using similar techniques. Wenzler *et al.* (2006) modeled the VIRGO TSI using Kitt Peak National Observatory (KPNO) magnetograms. They found an R^2 as high as 0.83. Withbroe (2009) used Michelson Doppler Imager (MDI) data to model the composite VIRGO TSI and obtained an R^2 of 0.76.

In summary, precision ground-based photometry, by accurately removing TSI variations caused by solar activity, can help reveal differences between space-based TSI measurements.

Acknowledgements We thank the students and staff for their efforts in helping to obtain the daily photometric images used in this study. This research was partially supported by NSF Grant ATM-0848518 and NASA Grants NNX11AB51G and NNX11AK46G.

References

- Ball, W.T., Unruh, Y.C., Krivova, N.A., Solanki, S.K., Harder, J.W.: 2011, *Astron. Astrophys.* **530**, 71.
- Ball, W.T., Unruh, Y.C., Krivova, N.A., Solanki, S., Wenzler, T., Mortlock, D.J., Jaffe, A.H.: 2012, *Astron. Astrophys.* **541**, 27.
- Bevington, P.R., Robinson, D.K.: 1992, *Data Reduction and Error Analysis for the Physical Sciences*, McGraw-Hill, New York, 208.
- Chapman, G.A., Dobias, J.J., Arias, T.: 2011, *Astrophys. J.* **728**, 150.
- Chapman, G.A., Cookson, A.M., Preminger, D.G.: 2012, *Solar Phys.* **276**, 35.
- Chapman, G.A., Herzog, A.D., Lawrence, J.K., Walton, S.R., Hudson, H.S., Fisher, B.M.: 1992, *J. Geophys. Res.* **97**, 8211.
- Chapman, G.A., Cookson, A.M., Dobias, J.J., Preminger, D.G., Walton, S.R.: 2004, *Adv. Space Res.* **34**, 262.
- de Toma, G., White, O.R., Chapman, G.A., Walton, S.R., Preminger, D.G., Cookson, A.M.: 2004, *Astrophys. J.* **609**, 1140.
- Dewitte, S., Crommelynck, D., Mekaoui, S., Jonkoff, A.: 2004, *Solar Phys.* **224**, 209.
- Ermolli, I., Berrilli, F., Florio, A.: 2003, *Astron. Astrophys.* **412**, 857.
- Fontenla, J., Harder, J.: 2005, *Mem. Soc. Astron. Ital.* **76**, 826.
- Fontenla, J., White, O.R., Fox, P.A., Avrett, E.H., Kurucz, R.L.: 1999, *Astrophys. J.* **518**, 480.
- Fontenla, J.M., Curdt, W., Habereiter, M., Harder, J., Tian, H.: 2009, *Astrophys. J.* **707**, 482.
- Fröhlich, C.: 2003, In: Wilson, A. (ed.) *Solar Variability as an Input to the Earth's Environment, International Solar Cycle Studies (ISCS) Symposium, ESA SP-535*, 183.
- Fröhlich, C.: 2004, In: Pap, J.M., Fox, P. (eds.) *Solar Variability and Its Effects on Climate, AGU Geophys. Monogr.* **141**, 97.
- Fröhlich, C.: 2006, *Space Sci. Rev.* **125**, 53.
- Fröhlich, C., Anderson, B.N., Appourchaux, T., Berthomieu, G., Crommelynck, D.A., Domingo, V., *et al.*: 1997, *Solar Phys.* **170**, 1.
- Harvey, K.L., White, O.R.: 1999, *Astrophys. J.* **515**, 812.
- Jones, H.P., Chapman, G.A., Pap, J.M., Preminger, D.G., Turmon, M.J., Walton, S.R.: 2008, *Solar Phys.* **248**, 323.

- Kopp, G., Lawrence, G., Rottman, G.: 2005, *Solar Phys.* **230**, 129.
- Krivova, N.A., Solanki, S.K., Fligge, M., Unruh, Y.C.: 2003, *Astron. Astrophys.* **399**, L1.
- Li, K.J., Feng, W., Xu, J.C., Gao, L.S., Yang, L.H., Liang, H.F., Zahn, L.S.: 2012, *Astrophys. J.* **747**, 135.
- Livingston, W.C., Gray, D., Wallace, L., White, O.R.: 2005, In: Sankarsubramaniam, K., Penn, M., Pevtsov, A. (eds.) *Large-Scale Structures and Their Role in Solar Activity*, *ASP Conf. Ser.* **346**, 353.
- Mekaoui, S., Dewitte, S.: 2008, *Solar Phys.* **247**, 203.
- Mekaoui, S., Dewitte, S., Conscience, C., Chevalier, A.: 2010, *Adv. Space Res.* **45**, 1393.
- Preminger, D.G., Walton, S.R., Chapman, G.A.: 2001, *Solar Phys.* **202**, 53.
- Preminger, D.G., Walton, S.R., Chapman, G.A.: 2002, *J. Geophys. Res.* **107**, 1354.
- Solanki, S.K., Krivova, N.A.: 2004, *Solar Phys.* **224**, 197.
- Ulrich, R.K., Parker, D., Bertello, L., Boyden, J.: 2010, *Solar Phys.* **261**, 11.
- Walton, S.R., Chapman, G.A., Cookson, A.M., Dobias, J.J., Preminger, D.G.: 1998, *Solar Phys.* **179**, 31.
- Wenzler, T., Solanki, S.K., Krivova, N.A.: 2009, *Geophys. Res. Lett.* **36**, 11102.
- Wenzler, T., Solanki, S.K., Krivova, N.A., Fluri, D.M.: 2004, *Astron. Astrophys.* **427**, 1031.
- Wenzler, T., Solanki, S., Krivova, N.A., Fröhlich, C.: 2006, *Astron. Astrophys.* **460**, 583.
- Willson, R.C.: 2004, 35th COSPAR Scientific Assembly, Abstract No. 4451.
- Willson, R.C.: 2011, 2011 SORCE Science Meeting, <http://lasp.colorado.edu/sorce/news/2011ScienceMeeting>.
- Willson, R.C., Mordvinov, A.V.: 2003, *Geophys. Res. Lett.* **30**, 1199.
- Withbroe, G.L.: 2009, *Solar Phys.* **257**, 71.